The structure of parallel layers in steady two-dimensional magnetohydrodynamic flows in sudden duct expansions and contractions

Aleksandrova, S. and Molokov, S.

The structure of parallel layers in steady two-dimensional magnetohydrodynamic flows in sudden duct expansions and contractions

S. Aleksandrova and S. Molokov
Applied Mathematics Research Centre, Coventry University,
Priory Street, Coventry CV1 5FB, United Kingdom

May 7, 2010

Abstract. The structure of non-linear, steady, two-dimensional parallel layers at high values of the Hartmann number, Ha, the Reynolds number, Re, and the interaction parameter, N, for duct expansions and contractions has been investigated. The magnetic field is transverse to the flow. For the flow regime, in which the electromagnetic force balances the inertial force in the layer, a viscous sublayer at the solid wall parallel to the magnetic field has been obtained, in which the flow is driven by the pressure gradient induced in the outer, inviscid layer.

Keywords: magnetohydrodynamics, boundary layers, high magnetic field

PACS: 47.35.Tv, 47.65.-d

1 Introduction

Magnetohydrodynamic (MHD) flows are of great importance to liquid metal blankets for fusion reactors [1]. At the entrance a duct feeding liquid metal to the blanket expands into a larger one, which is followed by a manifold of ducts cooling the plasma chamber and/or breeding tritium. At the exit from the blanket there is a sudden contraction of a duct. The flows in the expansion and contraction regions greatly influence the global flow distribution and ultimately heat and mass transfer in cooling (or breeding) ducts and thus affect the efficiency of the whole blanket [2], [3].

Although flows in fusion applications are in general 3-D, here we will be interested in a simplified problem of 2-D expansions and contractions in the presence of a transverse magnetic field. We pursue the following aim: to investigate the asymptotic structure of the so-called parallel layers [4], [5] (figure 1) formed in a high magnetic field at the junction between narrow and wide channels. We will be particularly interested in the case when the flow in layer P is governed by the electromagnetic-inertia interaction, which is important not only for expansions but in a wider context of MHD flows in high magnetic field.

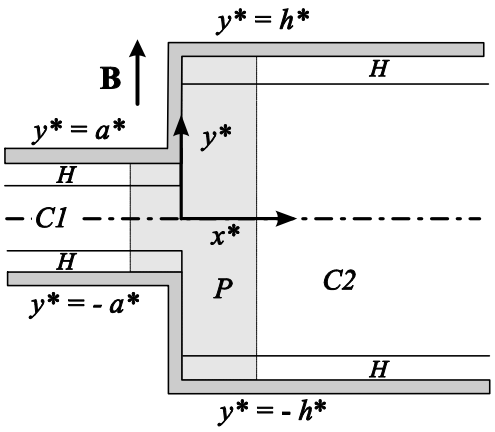

Figure 1: Schematic diagram of the flow in an expansion and main flow subregions in a high magnetic field: cores $C1$ and $C2$, Hartmann layers H, and parallel layer P.

2 Formulation

We will be concerned with the steady, 2-D flow of a viscous, electrically conducting, incompressible fluid in the plane (x, y) in a sudden expansion or a sudden contraction in the presence of a strong, uniform, transverse, external magnetic field $\mathbf{B}_0 = B_0\hat{\mathbf{y}}$ (Fig. 1). The walls of the narrow and wide channels are separated by distances $2a^*$ and $2h^*$, respectively, yielding the aspect ratio of $h = h^*/a^*$. The junction between the narrow and wide channels is located at $x = 0$.

The dimensionless, steady, inductionless equations governing the flow are [5], [4]:

$$Ha^{-2}\nabla^2\mathbf{v} - \mathbf{v}\cdot\hat{\mathbf{x}} = \nabla p + N^{-1}(\mathbf{v}\cdot\nabla)\mathbf{v}, \tag{1}$$

$$\nabla\cdot\mathbf{v} = 0, \tag{2}$$

where the length, the fluid velocity $\mathbf{v} = u\hat{\mathbf{x}} + v\hat{\mathbf{y}}$, and the pressure p are normalized by a^*, v_0, and $a^*\sigma v_0 B_0^2$, respectively; σ is the electrical conductivity of the fluid; v_0 is the average fluid velocity in the narrow channel.

The second term in Eq. (1) represents the Lorentz force, which in the case of a 2-D flow reduces to linear anisotropic damping affecting the axial component of momentum only. The constant electric field is incorporated into the pressure gradient. This corresponds to lateral walls being perfectly conducting and electrically short-circuited.

The dimensionless parameters in Eq. (1) are the Hartmann number, $Ha = B_0 a^*\sqrt{\sigma/\rho\nu}$, the square of which characterises the ratio of the electromagnetic to viscous forces, and the interaction parameter, $N = \sigma a^* B_0^2/\rho v_0$, which characterises the ratio of the electromagnetic to inertial forces in the narrow duct. Here ρ and ν are the density and kinematic viscosity of the fluid, respectively. The Reynolds number is expressed as follows: $Re = Ha^2/N$. In fusion reactor blankets $Ha \sim 10^3 - 10^5$, $N \sim 10^3 - 10^4$, $Re \sim 10^2 - 10^6$.

In the wide channel the electromagnetic parameters are higher, while the Reynolds number is the same. Indeed, introducing subscript h, gives: $Ha_h = B_0 h^* \sqrt{\sigma/\rho\nu} = hHa$, $N_h = \sigma h^{*2} B_0^2/\rho v_0 = h^2 N$, and $Re_h = Ha_h^2/N_h = Ha^2/N = Re$.

The boundary conditions are the no-slip-, and the fully-developed-flow- conditions, which yield:

$$\mathbf{v} = 0 \qquad \text{at all walls,} \tag{3}$$

$$v \to 0,\ \partial u/\partial x \to 0 \text{ as } x \to \pm\infty. \tag{4}$$

The average fluid velocity is fixed, i.e.

$$\frac{1}{2}\int_{-1}^{1} u(x<0)dy = \frac{1}{2h}\int_{-h}^{h} u(x>0)dy = 1. \tag{5}$$

3 Scaling

For $Ha \gg 1$ and $N \gg 1$ most of the flow domain is occupied by the inviscid and inertialess cores $C1$ for $x < 0$ and $C2$ for $x > 0$ (Fig. 1). Neglecting viscous and inertial terms in Eq. (1) and using Eq. (5) yields: $u_{C1} = 1$, $v_{C1} = 0$, $dp_{C1}/dx = -1$, and $u_{C2} = h^{-1}$, $v_{C2} = 0$, $dp_{C2}/dx = -h^{-1}$. Thus the flow in both cores remains fully developed up to the junction.

The cores $C1$ and $C2$ are separated from walls $y = \pm 1$ for $x < 0$ and $y = \pm h$ for $x > 0$, respectively, by the exponential Hartmann layers. The analysis of these layers is standard [6] and is not presented here.

At the junction there is an $O(1)-$jump in the x-component of the core velocity, which is smoothed out in the parallel layer P (Fig. 1). The thickness of this layer and the events at the parallel walls at $x = 0$, $|y| > 1$ are the main concern of this paper.

We introduce scaling for layer P as follows: $u = u_P$, $v = \delta^{-1} v_P$, $p = \delta p_P$, $\xi = \delta^{-1} x$, where δ ($\gg Ha^{-1}$, $\gg N^{-1}$) is the thickness of the layer, and quantities with subscript P are $O(1)$. Substituting this scaling into Eqs. (1) and (2), and neglecting terms of smaller order with respect to those retained yields :

$$u_P = -\frac{\partial p_P}{\partial \xi}, \tag{6}$$

$$\frac{\partial u_P}{\partial \xi} + \frac{\partial v_P}{\partial y} = 0, \tag{7}$$

$$\frac{1}{Ha^2\delta^4}\frac{\partial^2 v_P}{\partial \xi^2} = \frac{\partial p_P}{\partial y} + \frac{1}{N\delta^3}\left\{u_P\frac{\partial v_P}{\partial \xi} + v_P\frac{\partial v_P}{\partial y}\right\}. \tag{8}$$

Equation (6) implies that the axial pressure gradient balances the electromagnetic force for all values of δ. Concerning Eq. (8), three cases are possible depending on the relation between Ha and N.

Case I. For $N \gg Ha^{3/2}$ the balance in Eq. (8) is between the electromagnetic and viscous forces, which yields $\delta = Ha^{-1/2}$. Note that the electromagnetic force enters the balance indirectly, via the $y-$component of the pressure gradient.

Case II. For $N \ll Ha^{3/2}$ the balance is electromagnetic-inertial, which gives $\delta = N^{-1/3}$.

Case III. Finally, for $N = O(Ha^{3/2})$, all the three forces are in balance, which yields $\delta = Ha^{-1/2} = \alpha N^{-1/3}$, where $\alpha = Ha^{3/2}N^{-1}$.

Notice that the scaling for the layer thickness is the same as for duct expansions being linear functions of x [7]. However, the magnitude of the velocity is different. In all the three cases, the flow is diverted in the $\pm y-$direction by the $y-$component of the pressure gradient to form jets in the $\pm y-$direction of magnitude δ^{-1}.

The analysis for *Case II* is yet incomplete. As the main balance in layer P is inviscid, there must be a viscous sublayer, PS, at the solid walls at $x = 0$. Let γ be the thickness of the sublayer. Introducing scaling for the sublayer, $u = \gamma N^{1/3} u_{PS}$, $v = N^{1/3} v_{PS}$, $p = N^{-1/3} p_P(x = 0) + \gamma^2 N^{1/3} p_{PS}$, $\zeta = \gamma^{-1} x$, and keeping leading terms as $Ha, N \to \infty$ yields

$$\frac{N^{1/3}}{Ha^2\gamma^2}\frac{\partial^2 v_{PS}}{\partial \zeta^2} = \frac{1}{N^{1/3}}\left.\frac{dp_P}{dy}\right|_{x=0} + \frac{1}{N^{1/3}}\left\{u_{PS}\frac{\partial v_{PS}}{\partial \zeta} + v_{PS}\frac{\partial v_{PS}}{\partial y}\right\}.$$

The balance between all the three terms gives the thickness of the sublayer:

$$\gamma = \frac{N^{1/3}}{Ha} = \frac{1}{(HaRe)^{1/3}}. \tag{9}$$

Note that the flow in the sublayer is driven by the $y-$component of the pressure gradient induced by the flow in the outer, inviscid layer P.

4 Results and discussion

The problem defined by Eqs. (1) - (5) has been solved numerically using the commertial, finite-volume code CFX [8]. Typical computational mesh consists of 160 points in the $x-$ and 320 points in the $y-$ direction. The grid is nonuniform, clustered at the Hartmann walls and in the parallel layers with the minimum grid spacing of 5×10^{-5}. There are 8-10 points in layers H and the sublayer SP each. The code has been verified on the results for the non-magnetic case [9], which include bifurcations to the asymmetric solutions. An excellent agreement has been achieved.

We employed time-stepping until convergence to a steady flow. No 2-D instabilities have been observed for the range of parameters used here. 3-D instabilities of the jets in the parallel layers have not been studied. They are possible but do not necessarily occur [10].

The results for a 1:4 expansion are shown in Figs. 2-8. Figure 2 shows the streamlines in the inertialess flow (*Case I*) for $Re = 0$, $Ha = 10^3$ ($Ha^{3/2} = 31623$, $N = \infty$). There are no separation zones and the flow is symmetric about

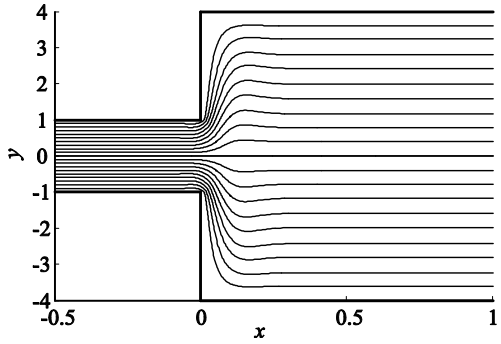

Figure 2: Streamilnes in the inertialess flow for $Ha = 10^3$.

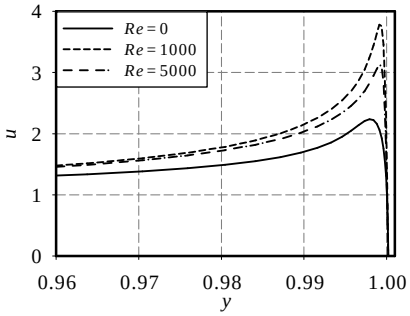

Figure 3: Axial jets at $x = 0$ for $Ha = 10^3$, and for several values of Re.

the axis $y = 0$. The pressure gradient diverts the fluid into the $\pm y-$direction in a parallel layer of thickness $O(Ha^{-1/2})$. The magnitude of velocity in the jet is $O(Ha^{1/2})$. Before the junction there is a slight outflow of the fluid away from the Hartmann walls into the core. Then, as the fluid needs to fill the wide channel right after the corners at $y = \pm 1$, $x = 0$, small axial jets develop at the Hartmann walls in the narrow channel region as shown in Fig. 3.

At $Re = 1620$ ($N = 617$) first pair of separation zones appears (Fig. 4). What is interesting is that they are born not at the corners of an expansion but at the parallel walls, at $y = \pm 3.2$ (5a). As Re increases their size increases as well and at $Re = 1670$ ($N = 599$) the ends of the separation zones reach the outer corners at $y = \pm 4$ (5b). For $Re = 2300$ ($N = 435$) a second pair of the separation zones appear at corners at $y = \pm 1$. Typical streamlines in this case are shown in Fig. 5c for $Re = 6600$ ($N = 152$) and $y \geq 0$. For $Re = 6950$ ($N = 144$) the two pairs of separation zones merge and a single pair remains, beginning at $y = \pm 1$ and ending at $y = \pm 4$.

The thickness of the parallel layer P is obtained by the projection of the slope at the inflexion point of the jet onto the axis. The results are shown in Fig. 6 for $y = 2.57$ and $Ha = 10^3$. It is seen that the thickness becomes proportional to $N^{-1/3}$ for $N < 1000$ as expected from the scaling analysis. Similar profiles

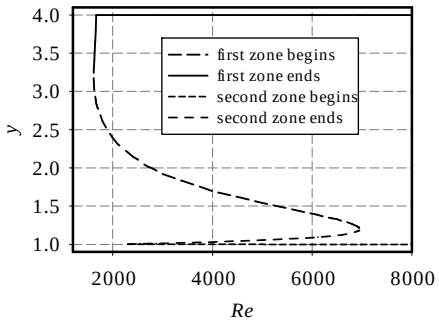

Figure 4: Positions of the beginning and the end of separation zones for $Ha = 10^3$ against Re.

may be obtained for different values of Ha and y.

The thickness of the inner sublayer has been determined indirectly by the behaviour of friction at the vertical wall. From scaling for the sublayer with (9) follows that $\frac{\partial v}{\partial x}(x = 0) \sim Ha$ independent of the Reynolds number. Figure 7 shows that for $Re = 10^4$ the linear dependence on Ha is achieved for $|y| \leq 1.5$ close to the inner corners of the duct where the recirculating flow is strong. For $|y| > 1.5$ a much higher value of Re is required to get the sublayer with viscous-inertia balance. The dependence of friction on Re is shown in Fig. 8. The friction becomes independent of Re as Re increases, as predicted.

The results for a 4:1 contraction are shown in Figs. 2, 6, 9 and 10. It is seen that the thickness of layer P is proportional to $N^{-1/3}$ for $N < 2000$ (Fig. 6) and that friction linearly varies with Ha and is independent of Re (Figs. 9 and 10), which proves the existence of sublayer PS.

In conclusion, electromagnetic-inertia balance is dominant in the parallel layer. Viscous sublayer exists at the parallel walls in most cases studied here. The flow in the sublayer is driven by the pressure gradient in layer P.

References

[1] L. Bühler, "Liquid metal magnetohydrodynamics for fusion blankets," in: *Magnetohydrodynamics: Historical Evolution and Trends* (S. Molokov, R. Moreau, H.K. Moffatt, eds). Springer, 171 (2007).

[2] J. Reimann, L. Bühler, C. Mistrangelo, and S. Molokov, "Magnetohydrodynamic issues of the HCLL blanket," Fusion Engineering and Design **81**, 625 (2006).

[3] C. Mistrangelo, "Three-dimensional MHD flow in sudden duct expansions," *Forschungszentrum Karlsruhe Report*, FZKA 7201 (2006).

[4] U. Müller and L. Bühler, *Magnetohydrodynamics in Channels and Containers*, Springer (2001).

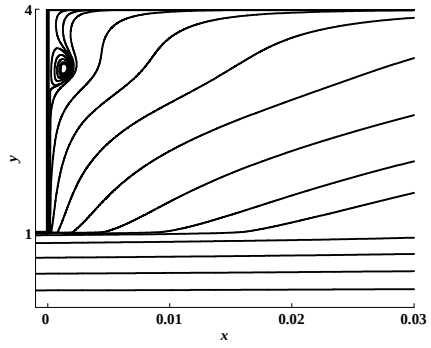

a)

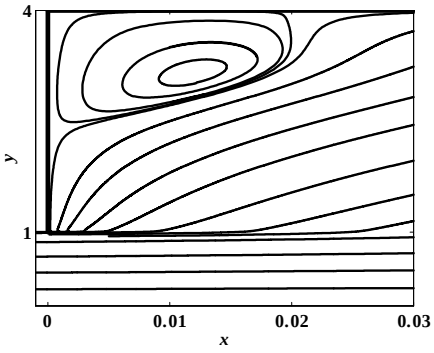

b)

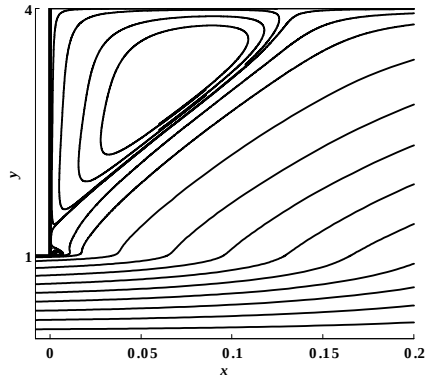

c)

Figure 5: Flow in an expansion for $Ha = 1000$, $y > 0$, and for $Re = 1650$ (a), 2000 (b), and 6600 (c).

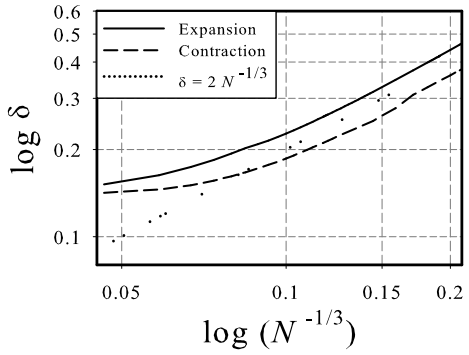

Figure 6: Thickness of the outer layer for $Ha = 10^3$ and for $y = 2.57$.

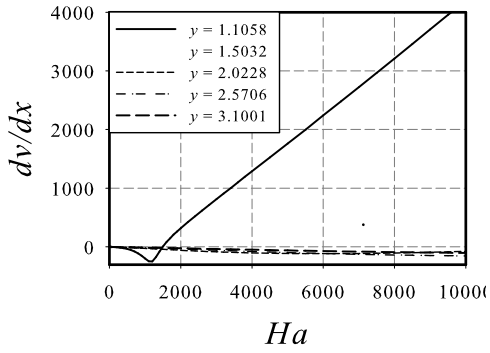

Figure 7: Variation of friction at the parallel wall with Ha for $Re = 10^4$ for an expansion at various positions.

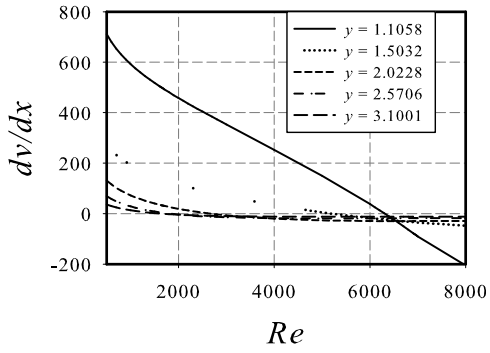

Figure 8: Variation of friction at the parallel wall with Re for $Ha = 10^3$ for an expansion at various positions.

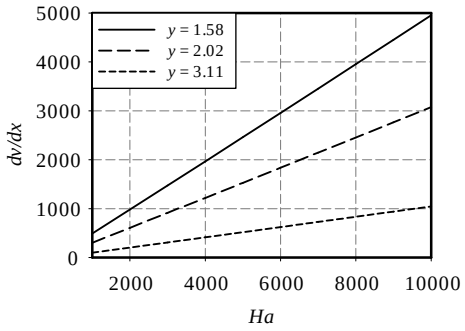

Figure 9: Variation of friction at the parallel wall with Ha for $Re = 10^4$ for a contraction at various positions.

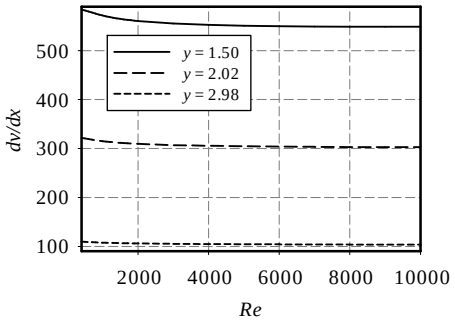

Figure 10: Variation of friction at the parallel wall with Re for $Ha = 10^3$ for a contraction at various positions.

[5] S. Molokov, "Two-dimensional parallel layers at high Ha, Re and N," in *Proc. 4^{th} pamir international conference on magnetohydrodynamics, France, 2000*, 153 (2000).

[6] R. Moreau and S. Molokov, "Julius Hartmann and his followers: a review on the properties of the Hartmann layer," in: *Magnetohydrodynamics: Historical Evolution and Trends* (S. Molokov, R. Moreau, H.K. Moffatt, eds). Springer, 155 (2007).

[7] J. C. R. Hunt and S. Leibovich, "Magnetohydrodynamic flow in channels of variable cross-section with strong transverse magnetic fields," J. Fluid Mech. **28**, 241 (1967).

[8] S. Aleksandrova, S. Molokov and, C. B. Reed "Modelling of liquid metal duct and free-surface flows using CFX," *Argonne National Laboratory Report*, ANL/TD/TM02-30 (2002) .

[9] N. Alleborn, K. Nandakumar, H. Raszillier and F. Durst, "Further contributions on the two-dimensional flow in a sudden expansion," J. Fluid Mech. **330**, 169 (1997) .

[10] R. Stieglitz, L. Barleon, L. Bühler and S. Molokov, "Magnetohydrodynamic flow in a right angle bend in a strong magnetic field," J. Fluid Mech. **326**, 91 (1996).